1964

Single crystal elastic constants of indium-thallium alloys

Donald Bob Novotny
Iowa State University

SINGLE CRYSTAL ELASTIC CONSTANTS OF INDIUM-THALLIUM ALLOYS

by

Donald Bob Novotny

A Dissertation Submitted to the

Graduate Faculty in Partial Fulfillment of

The Requirements for the Degree of

DOCTOR OF PHILOSOPHY

Major Subject: Physical Chemistry

Approved:

Signature was redacted for privacy.

In Charge of Major Work

Signature was redacted for privacy.

Head of Major Department

Signature was redacted for privacy.

Dean of Graduate College

Iowa State University
Of Science and Technology
Ames, Iowa

1964

TABLE OF CONTENTS

INTRODUCTION

The equilibrium phase diagram of the indium-thallium system, Figure 1, shows the phases which have the crystal structures of face-centered tetragonal, f.c.t., face-centered cubic, f.c.c., body-centered cubic b.c.c., and hexagonal closest packed, h.c.p. Contributions to this phase diagram have been made by many investigators and are summarized by Hansen (1). Three of the phases of this system are related through the transformations they undergo. The f.c.c. → f.c.t. transformation shown in Figure 1 has been investigated by Burkart and Read (2), and Basinski and Christian (3) who have established that this is a martensitic transformation. Also, Bridgman (4) has shown that thallium undergoes an allotropic transformation at approximately 40 kbars which was shown to be a h.c.p. → f.c.c. transformation by Meyerhoff and Smith (5). The elastic constants of the f.c.c. phase were measured as a function of composition and temperature with the anticipation that the results and the previously measured elastic constants of indium (6) and thallium (7) would yield information about the relative stabilities of the f.c.c., f.c.t., and h.c.p. phases.

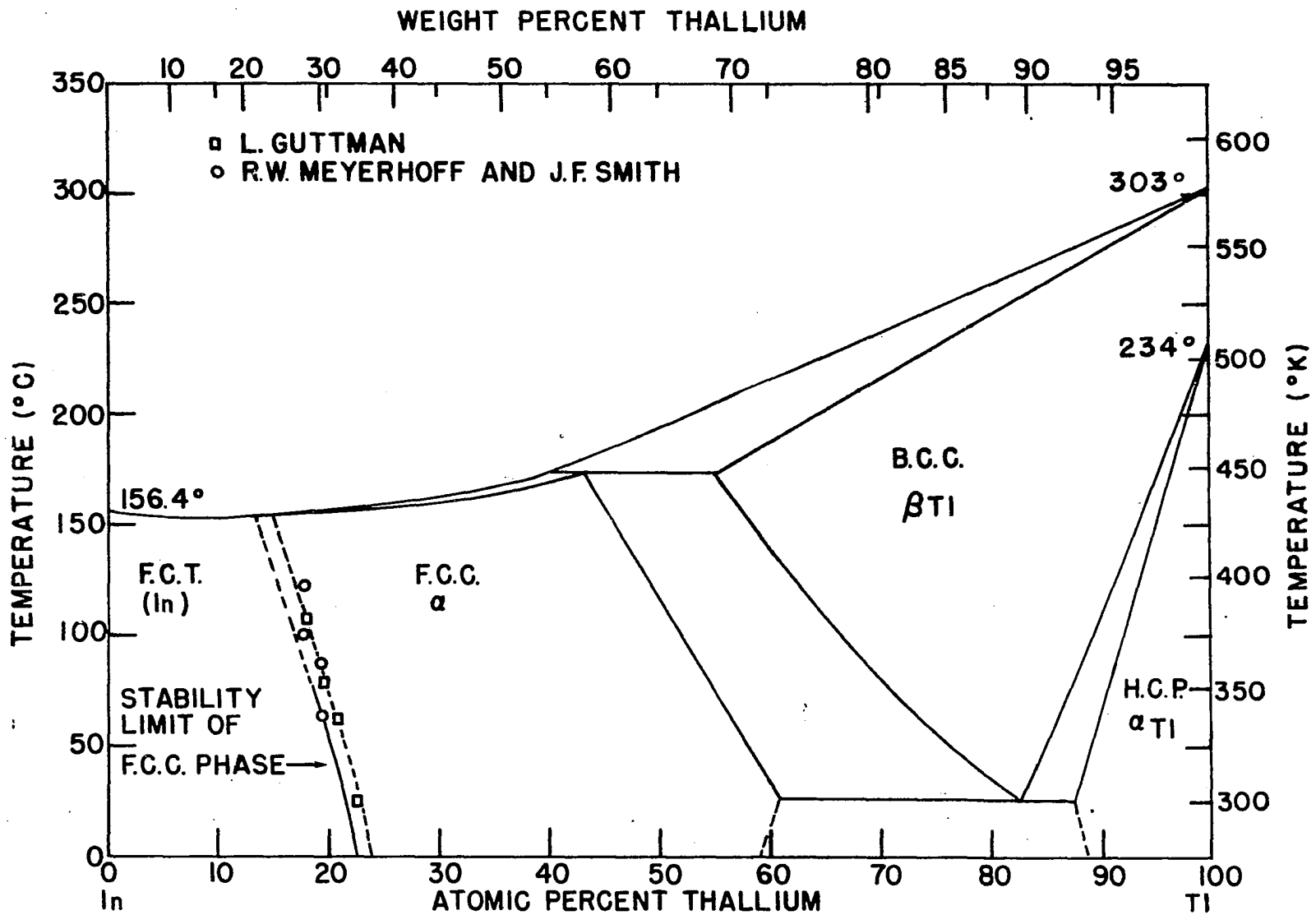

Figure 1. The indium-thallium phase diagram

Crystal Elasticity

For the purpose of introducing and defining symbols and concepts the subject of crystal elasticity will be reviewed. More extensive treatments of this subject may be found in the books by Kittel (8) and Nye (9). The strains in a crystal are defined in terms of the displacements u, v, and w and the positional coordinates x, y and z by the equations

$$e_1 = \partial u/\partial x,\ e_2 = \partial v/\partial y,\ e_3 = \partial w/\partial z,$$
$$e_4 = \partial v/\partial z + \partial w/\partial y,\ e_5 = \partial u/\partial z + \partial w/\partial x, \tag{1}$$

and

$$e_6 = \partial u/\partial y + \partial v/\partial x.$$

A force acting on a unit area in a solid is defined as a stress. When a crystal is in static equilibrium there are six independent stress components that may act upon it which will be denoted by the symbol T_i where i has the values from 1 to 6. In this notation the values of the index i represent two directions according to the scheme

$$1 \rightarrow xx,\ 2 \rightarrow yy,\ 3 \rightarrow zz,\ 4 \rightarrow yz,\ 5 \rightarrow xz,\ 6 \rightarrow xy \tag{2}$$

where the first direction indicates the direction of the force and the second the normal to the plane to which the force is applied. Hooke's law states that for small deformations the stress is proportional to the strain, so that the stress com-

ponents are linear functions of the strain components. These linear functions may be expressed by the equations

$$T_i = C_{ij}e_j \qquad (i,j = 1,2...6). \tag{3}$$

The number of independent elastic constants may be reduced from 36, as shown in Equation 3, to only 3 for a crystal with cubic symmetry by energy density and crystal symmetry considerations. The incremental work done on a crystal per unit volume when a stress acts through a strain is

$$dW = T_i de_i = C_{ij}e_j de_i \qquad (i,j = 1,2...6). \tag{4}$$

When an adiabatic process is considered the first law of thermodynamics may be written as

$$dE = dW, \tag{5}$$

where E is the internal energy of the solid. From these two relations it is seen that

$$\partial^2 E/ \partial e_j \partial e_i = C_{ij} \qquad (i,j = 1,2...6). \tag{6}$$

Since E is a thermodynamic function of state the value of the elastic constant does not depend on the order of differentiation of E and it can be seen that

$$C_{ij} = C_{ji} \qquad (i,j = 1,2...6). \tag{7}$$

Equation 7 reduces the number of independent elastic constants from 36 to 21. This number may further be reduced by the symmetry constraints of the respective crystal classes (9,10).

For cubic crystals there are only three independent elastic constants and they can be represented by the matrix

$$(C_{ij}) = \begin{bmatrix} C_{11} & C_{12} & C_{12} & 0 & 0 & 0 \\ C_{12} & C_{11} & C_{12} & 0 & 0 & 0 \\ C_{12} & C_{12} & C_{11} & 0 & 0 & 0 \\ 0 & 0 & 0 & C_{44} & 0 & 0 \\ 0 & 0 & 0 & 0 & C_{44} & 0 \\ 0 & 0 & 0 & 0 & 0 & C_{44} \end{bmatrix}. \quad (8)$$

Elastic constants may be related to the velocities of acoustic plane waves in a straightforward manner as shown in the review article by de Launay (11). Plane acoustic waves which are either pure longitudinal or pure transverse may only be propagated in the <110>, <100> and <111>-directions in a cubic crystal. Waves propagating in directions other than these are composed of longitudinal and transverse components. Three independent acoustic waves, one longitudinal and two transverse, may be propagated in the <110>-directions; the transverse waves propagating in the <100> and <111>-directions are degenerate. Because of this the most direct method of determining the values of the cubic elastic constants is to measure the sonic velocities in one of the <110>-directions.

Measurements of the velocities in other crystallographic directions may be used as a check on the values of the elastic constants.

EXPERIMENTAL PROCEDURE

Acoustic Measurements

The acoustic velocities were measured using the ultrasonic pulse-echo technique. This method has been described by Huntington (12), Lazarus (13) and Eros and Reitz (14). In essence this technique consists of transmitting a short pulse of high frequency acoustic energy through the sample and measuring the transit time of the pulse as it is reflected back and forth within the sample. The measurement of the transit time of the pulse is achieved by displaying the echo pattern on an oscilloscope. Pictures of a typical oscilloscope display may be found in the article by Eros and Reitz (14).

The values of the cubic elastic constants were determined from measurements of the velocities in both the [110] and [100] directions. Sonic velocities in the [110] direction are related to the elastic constants by Equations 9 which serve to define the cymbol C' and are:

$$\begin{aligned} \rho V_t^2 &= C_{44}, \\ \rho V_s^2 &= \tfrac{1}{2}(C_{11} - C_{12}) = C' \quad \text{and} \\ \rho V^2 &= \tfrac{1}{2}(C_{11} + C_{12} + 2C_{44}) \end{aligned} \tag{9}$$

where V_t is the velocity of a transverse wave polarized in the [001] direction, V_s is the velocity of a transverse wave

polarized in the $[1\bar{1}0]$ direction, V is the velocity of a longitudinal wave and ρ is the density. Because the transverse waves propagating in the $[100]$ direction are degenerate, velocities in this direction are related to only two elastic constants by Equations 10

$$\rho V_t = C_{44} \quad \text{and} \qquad \rho V_L = C_{11} \tag{10}$$

where V_L is the velocity of longitudinal wave. The values of the elastic constant C_{44} were determined from measurements of velocities in the $[110]$ direction and several checks were made by measuring velocities in the $[100]$ direction. The values of C_{11} were determined directly from measurements of velocities in the $[100]$ direction. These values were checked by measuring the values of the constant $\frac{1}{2}(C_{11} + C_{12} + 2C_{44})$ and using previously measured values of C_{44} and C' to calculate the values of C_{11}.

X and Y-cut transducers with a resonant frequency of 10 Mc/s were used to generate the acoustic pulses. These transducers were bonded to the single crystals with Nonaq Stopcock Grease. Thin bonds were made by heating an alloy single crystal on a hot plate to about 70°C, applying a small amount of grease to the crystal, placing a transducer on the crystal in the desired orientation and applying a firm even pressure

to the transducer as the crystal was cooled to room temperature.

Measurements of the acoustic velocities were made in temperature ranges which varied from 193 to 361°K. The high temperature limits were set by the highest temperature at which the leading edges of the pulses could be identified. At temperatures greater than room temperature the viscosity of the grease is small and energy transmission through the bond is difficult. This causes an appreciable attenuation in the observed pulses which distorts the echo pattern and makes it impossible to identify the leading edges of the pulses. The lower limits of the temperature ranges were determined by the temperatures at which the f.c.c. → f.c.t. transformations occurred. The velocity measurements were checked throughout the temperature ranges by making several measurements with different bonds and at room temperature by making measurements with phenyl salicylate bonds. Electrical contact to the quartz transducer was provided by placing the transducer adjacent to a flat copper contact plate in the sample holder.

Sample Preparation

Alloys of compositions 28.13, 30.16, 35.15 and 39.06 at. % Tl were prepared from indium and thallium with the

respective purities of 99.97% and 99.95% given by the suppliers. The indium was obtained from The Indium Corporation of America and the thallium from the American Refining and Smelting Company. Crucibles machined from high quality, nonporous graphite were used to prepare the alloys. At temperatures greater than room temperature the thallium oxidized rapidly in air which made it necessary to initially alloy the metals under an inert atmosphere. This was done by placing nominal amounts of indium and thallium in a graphite crucible, placing the crucible under a helium atmosphere and heating the crucible to a temperature in excess of 300°C. The homogeneity of the alloy was ensured by remelting and pouring the alloy from crucible to crucible in the air while a stream of helium was directed over the crucible mouths.

Alloy single crystals were grown using a modification of the Bridgman technique (15). This was done in the apparatus shown schematically in Figure 2. The procedure used for growing single crystals was as follows: the alloy was placed in the crucible, heated several degrees above its melting range, maintained at this temperature for several minutes to ensure complete melting and quenched. The quenching was effected by circulating water at ambient temperatures through the inlet

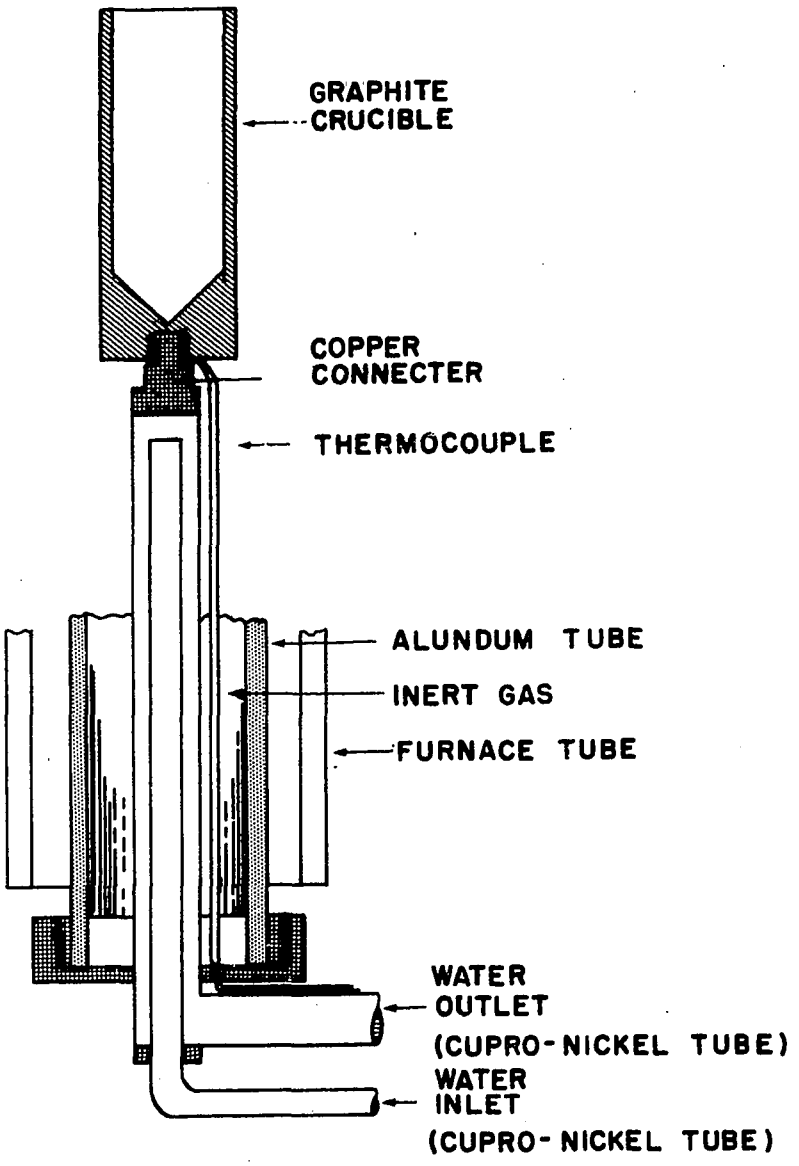

Figure 2. A schematic diagram of the apparatus used for growing single crystals

tube onto the base of the connector and through the outlet tube. The alloys were then etched in concentrated sulfuric acid and examined for grain boundaries. After several attempts to grow single crystals, ingots were usually obtained which contained only a few large grains from which single crystals would be cut. These ingots were annealed in a vacuum for a few days at 130°C to remove all internal stress.

Two single crystals were cut from the same grain in each alloy. The single crystals were aligned by back reflection Laue techniques and parallel faces were cut on a Sparcatron spark machine so acoustic waves could be propagated in the [110] direction in one crystal and the [100] direction in the other. The crystals were cut thin (approximately ½ cm) in the [110] direction to enable the measurement of the velocity associated with the constant C'. The value of C' was found to be extremely small and necessitated the measurements of long transit times between the echoes. The faces of the single crystals were made parallel to $\pm$ 0.0004 cm by carefully polishing them on 600 grit metallographic paper. Worked metal was removed from the crystals by etching with concentrated sulfuric acid and Laue photographs of these faces showed sharp spots indicating the absence of worked metal. Samples were taken

adjacent to each crystal face and analyzed for indium content; the results showed the alloys to be homogeneous to better than 0.1 at. % Tl.

RESULTS

The velocities were converted to the elastic constants with the densities calculated from the lattice parameters measured by Meyerhoff and Smith (5). The average mass per unit cell was determined from the alloy analysis and calculated with the assumption that these alloys are substitutional solid solutions and neither vacancies nor interstitial atoms exist. The respective densities are 8.649, 8.745, 8.983 and 9.168 g/cm^3 for the alloys of compositions 28.13, 30.16, 35.15 and 39.06 at. % Tl. The elastic constant data of each measured elastic constant for each alloy could be adequately represented in the temperature range of the measurements by the linear function

$$C = A + B(T - 273) \tag{11}$$

where C represents the value of a specific elastic constant of an alloy at the temperature T in degrees Kelvin. The values of A and B were determined by the method of least squares (16). The values of A and B along with their standard deviations, the root mean square deviations (RMSD) and the temperature ranges over which the measurements were made are given in Tables 1 through 3. The values of the elastic constants are plotted as a function of temperature in Figures 3 through 5.

Table 1. The linear representation of C_{44} in units of 10^{11} dyn/cm^2, $C_{44} = A + B(T - 273)$

At. % Tl	A	$-B \times 10^3$	RMSD	Temperature range in ^oK
28.13	0.841 ± 0.003	0.3 ± 0.2	0.003	277 - 300
30.16	0.869 ± 0.001	0.69 ± 0.04	0.002	273 - 330
35.15	0.889 ± 0.002	0.78 ± 0.05	0.005	204 - 300
39.06	0.892 ± 0.001	0.83 ± 0.03	0.004	193 - 301

Table 2. The linear representation of C_{11} in units of 10^{11} dyn/cm^2, $C_{11} = A + B(T - 273)$

At. % Tl	A	$-B \times 10^3$	RMSD	Temperature range in ^oK
28.13	4.022 ± 0.005	0.55 ± 0.12	0.011	206 - 298
30.16	4.105 ± 0.003	1.17 ± 0.07	0.012	203 - 361
35.15	4.101 ± 0.004	1.10 ± 0.09	0.008	203 - 297
39.06	4.110 ± 0.004	1.25 ± 0.10	0.014	198 - 347

Table 3. The linear representation of $C' = \frac{1}{2}(C_{11} - C_{12})$ in units of 10^{11} dyn/cm^2, $\frac{1}{2}(C_{11} - C_{12}) = A + B(T-273)$

At. % Tl	A	$-B \times 10^4$	RMSD	Temperature range in ^oK
28.13	0.0279 ± 0.0002	-0.4 ± 0.2	0.0004	274 - 299
30.16	0.0380 ± 0.0001	0.11 ± 0.06	0.0002	234 - 299
35.15	0.0619 ± 0.0003	0.92 ± 0.08	0.0005	207 - 300
39.06	0.0815 ± 0.0003	2.12 ± 0.08	0.0004	209 - 269

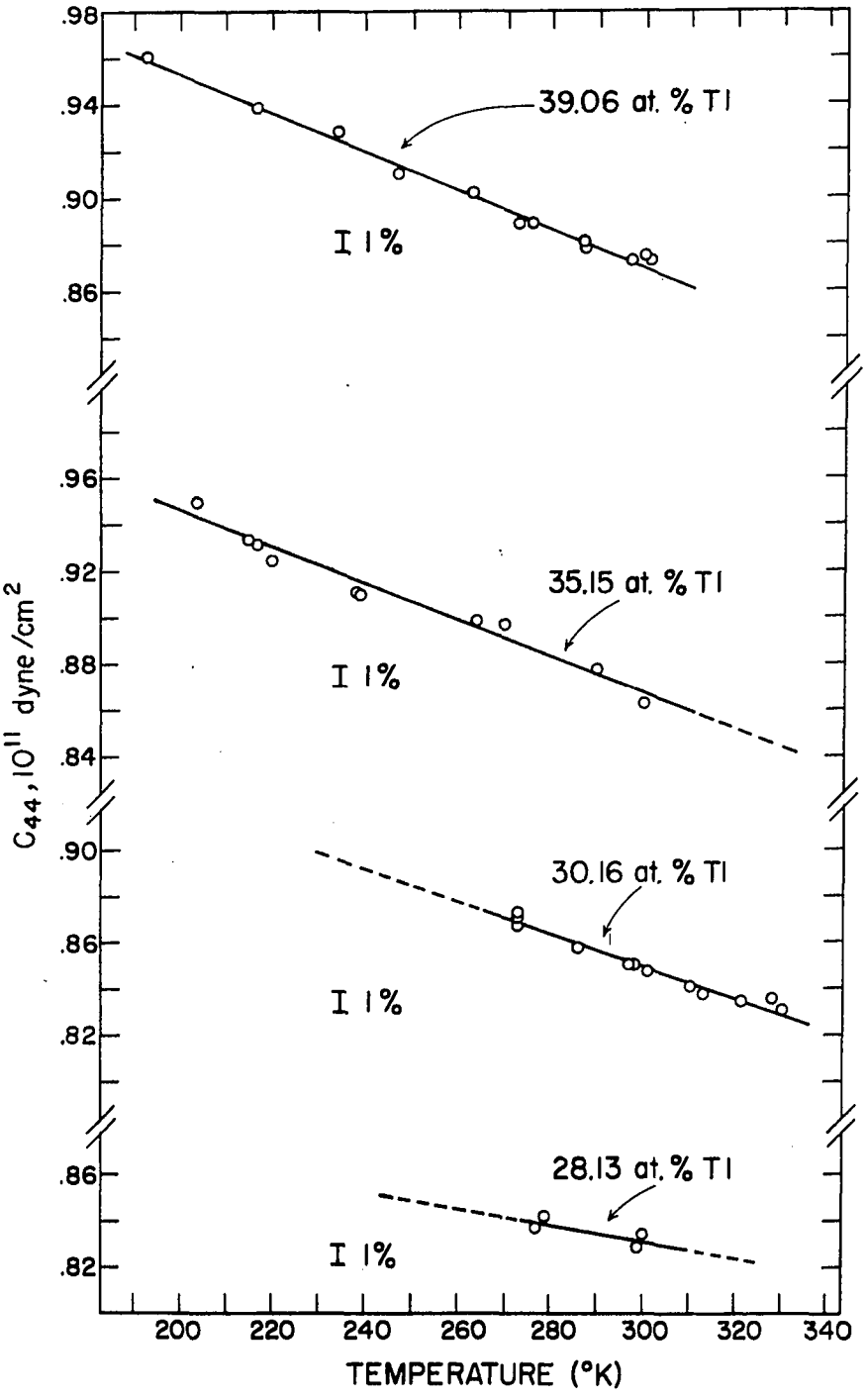

Figure 3. Linear representations of the elastic constant data for C_{44}

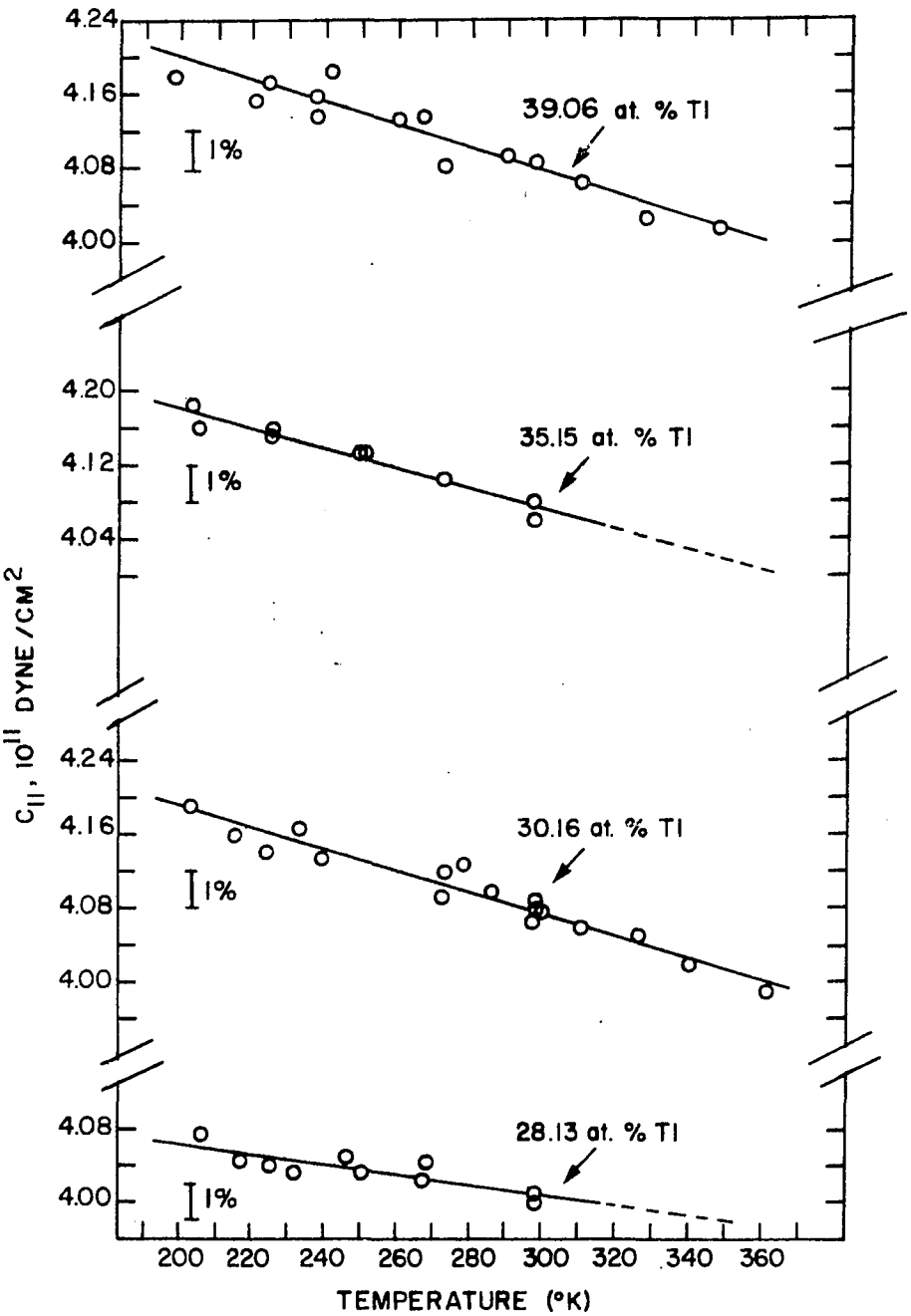

Figure 4. Linear representations of the elastic constant data for C_{11}

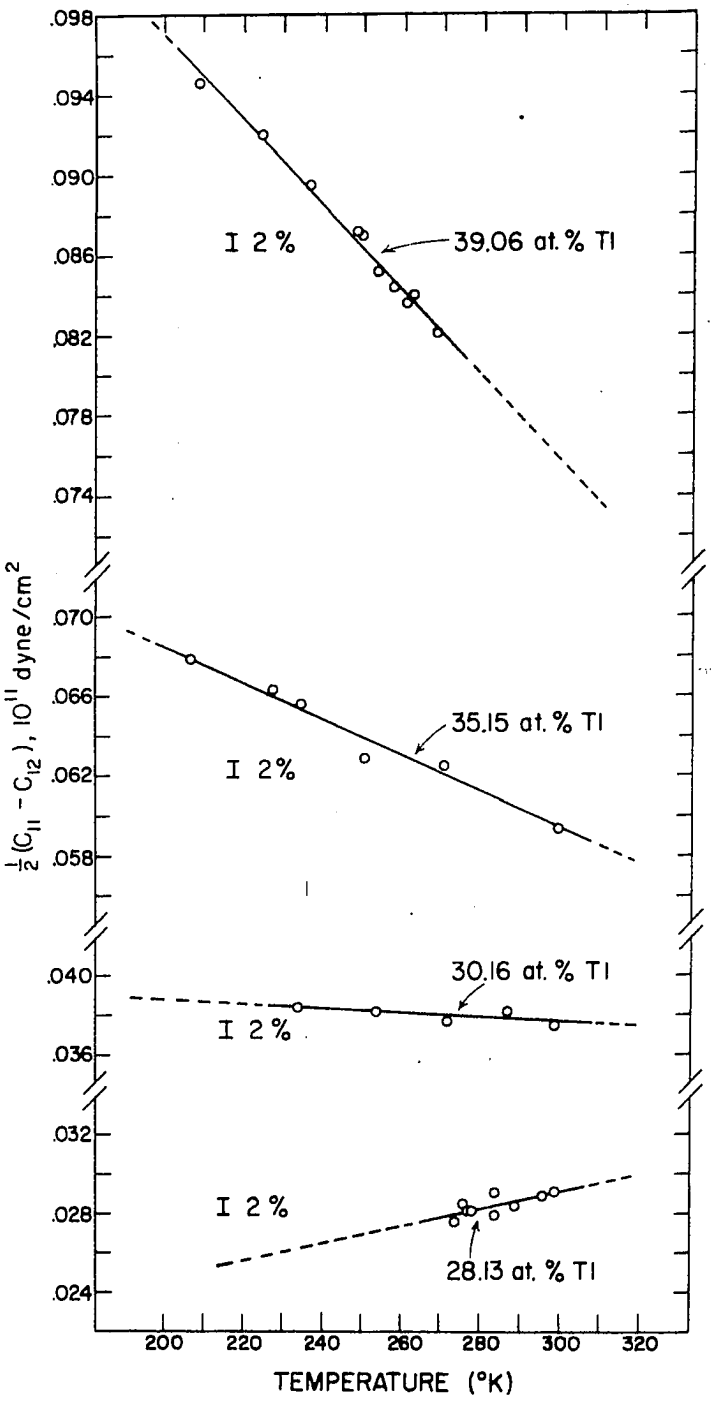

Figure 5. Linear representations of the elastic constant data for $\frac{1}{2}(C_{11} - C_{12}) = C'$

In addition to the random errors which are reflected by the scatter in the elastic constant data there are possible systematic errors which may affect the accuracy of the determination. A discrepancy of $\pm$ 0.05 at. % Tl in the composition would affect the density and would reflect an error in the values of the elastic constants of 0.01%. The reported values of the elastic constants are not corrected for thermal expansion because of the absence of any thermal expansion data for the alloys. These effects are estimated from the thermal expansion data for indium and thallium of Smith and Schneider (17) and Meyerhoff and Smith (18) respectively and change the values of the elastic constants by less than 0.5% of their values for each 100 degree temperature change. The possible errors introduced in the values of the elastic constants from a precision in the measurements of the crystal thickness of $\pm$ 0.0003 cm and the crystal faces having a parallelism to $\pm$ 0.0005 cm is less than 0.3%. The maximum estimated error is 0.3% at room temperature plus a 0.5% increase for each 100 degree change from room temperature.

The use of several different measurements to determine the values of the elastic constants and checks on these values by independent measurements reduce the possibility of system-

atic errors originating from nonparalled faces and dimensional measurements. This is because, in the process of remeasuring and checking the elastic constant values, these errors tend to become random errors and are reflected in the consistency between the different measured values. The value of the checks of C_{44} agreed to well within the consistency of the previously determined values of C_{44}. The values of the checks on C_{11}, which reflect all of the errors in the determined values of C_{44} and C', agreed to within 1% of the determined values of this constant.

DISCUSSION

Anisotropy and Phase Stability

The anisotropy ratio for a cubic crystal is defined as the ratio C_{44}/C'. For all the alloys which were investigated the anisotropy ratio is large and its value increases rapidly with decreasing thallium content. The plot in Figure 6 illustrates this behaviour. From the definition of the anisotropy ratio it is seen to be a comparison between the resistances of the crystal to the (110) $[001]$ and (110) $[1\bar{1}0]$ shears. The rapid increase of the anisotropy ratio with decreasing thallium content reflects the small values of C' and their rapid decrease with decreasing thallium content.

In general for any crystal to be stable its resistance to any independent shear must be positive definite, i.e. there must be a force resisting any independent shear deformation in the crystal. In particular for a cubic crystal to be mechanically stable the value of C' must be greater than zero. This may be seen simply from the fact that if C' were less than or equal to zero there would be no resistance to the (110) $[1\bar{1}0]$ shear. This argument was used to find an indium-rich stability limit of the f.c.c. phase field by extrapolating the values of C' to $C' = 0$.

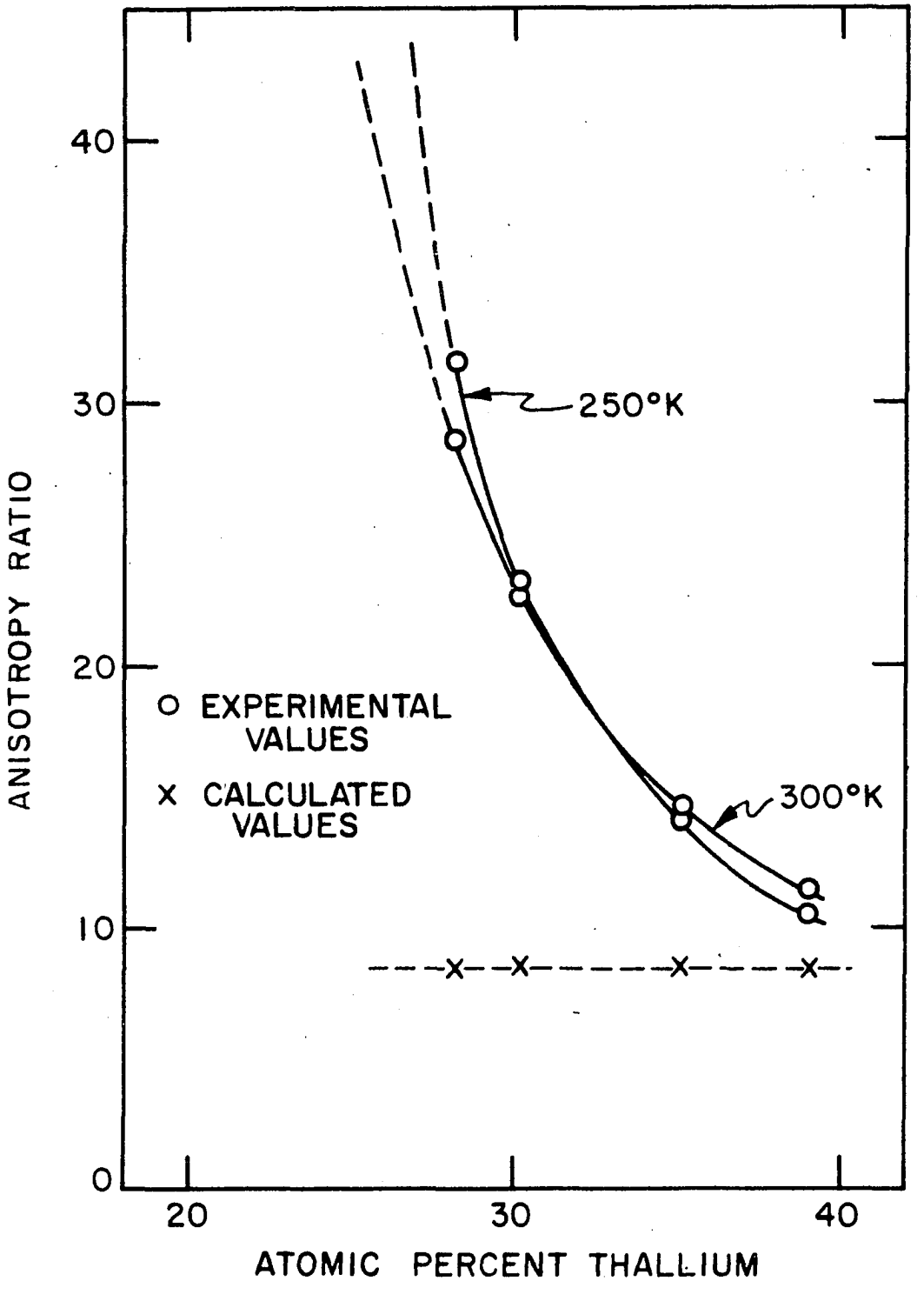

Figure 6. Graphical representation of the experimental and calculated values of the anisotropy ratio

The values of C' could be adequately represented at any temperature in the range of 198 to 348°K by the linear equation

$$C'(T) = A + Bx_{Tl}, \qquad (12)$$

where A and B are constants, x_{Tl} is the atomic per cent of thallium, and C'(T) is the elastic constant C' expressed as a function of composition at the temperature T. The values of the constants A and B were determined by the method of least squares (16) and are given for several temperatures in Table 4. Plots of Equation 12 for the different temperatures at which A and B were determined are shown in Figure 7. The alloy compositions at which C' = 0 at the different temperatures can be read directly from this figure, and the locus of these compositions is drawn on the phase diagram in Figure 1 with the label "stability limit of f.c.c. phase".

This stability limit extends toward higher thallium concentrations at lower temperatures. From the data of this investigation the terminus is indicated to be about 30 at. % Tl at 0°K. The f.c.c. phase is mechanically unstable and cannot exist on the indium-rich side of this stability limit. However, none of the existing data precludes the existence of the f.c.t. phase on the thallium-rich side of this stability limit. The fact that the experimental points of Guttman (19) and Meyerhoff and Smith (5) are close to this line indicates

that the value of C' is very small when the f.c.c. → f.c.t. transformation occurs. Thus, it may be concluded that alloy compositions greater than 30 at. % Tl are not likely to exist as the f.c.t. phase at low temperatures; this is in agreement with Guttman's findings (19) that a 25 at. % Tl alloy is tetragonal at liquid nitrogen temperatures while a 30 at. % Tl alloy is still cubic at these temperatures.

Table 4. Linear representation of C' as a function of composition in units of 10^{11} dyn/cm^2

	$C'(T) = A + Bx_{Tl}$	
Temperature ^{o}K	-A	B x 10^4
348	0.060 ± 0.004	32.2 ± 1.2
323	0.076 ± 0.003	37.7 ± 0.8
300	0.0914 ± 0.0008	42.8 ± 0.2
273	0.109 ± 0.001	48.8 ± 0.3
248	0.126 ± 0.003	54.4 ± 0.8
223	0.143 ± 0.005	60.1 ± 1.4
198	0.153 ± 0.008	63.7 ± 2.5

The vanishing of C' in the composition range of the f.c.c. → f.c.t. transformation is consistent with the double shear mechanism proposed for this transformation by Bowles, et al. (20) and Basinski and Christian (3). In this mechanism the atomic movements are equivalent to the two successive (101) $[10\bar{1}]$ and (110) $[1\bar{1}0]$ shears; these shears are those specifi-

cally associated with the elastic constant C'. The decrease in the value of C' as this transformation is approached is also consistent with Zener's interpretation (21) of the process of slip and transformation in terms of the free energy and shear strain. In Figure 8 the height of the potential barrier between the minima, which must be surmounted for the transformation to occur, correlates with the critical resolved shear stress required for the transformation; the curvatures near the minima represent the shear constants. The curves T_1, T_2, and T_3 represent the proposed effect of the temperature and show how the parent phase first becomes metastable and then unstable as the temperature decreases. It can be seen from this picture that the curvatures at the minimum positions of the free energy curves for the stable parent phase decrease as the M_s temperature is approached. Therefore, it is expected that the elastic modulus of the parent phase should decrease as the temperature is lowered to the M_s temperature and be very small or zero at this temperature; this is exactly what is observed. Further evidence for the validity of this picture is provided by Burkart and Read (2) who found that an application of stress in the elastic region raises the M_s temperature. This is predicted from this picture.

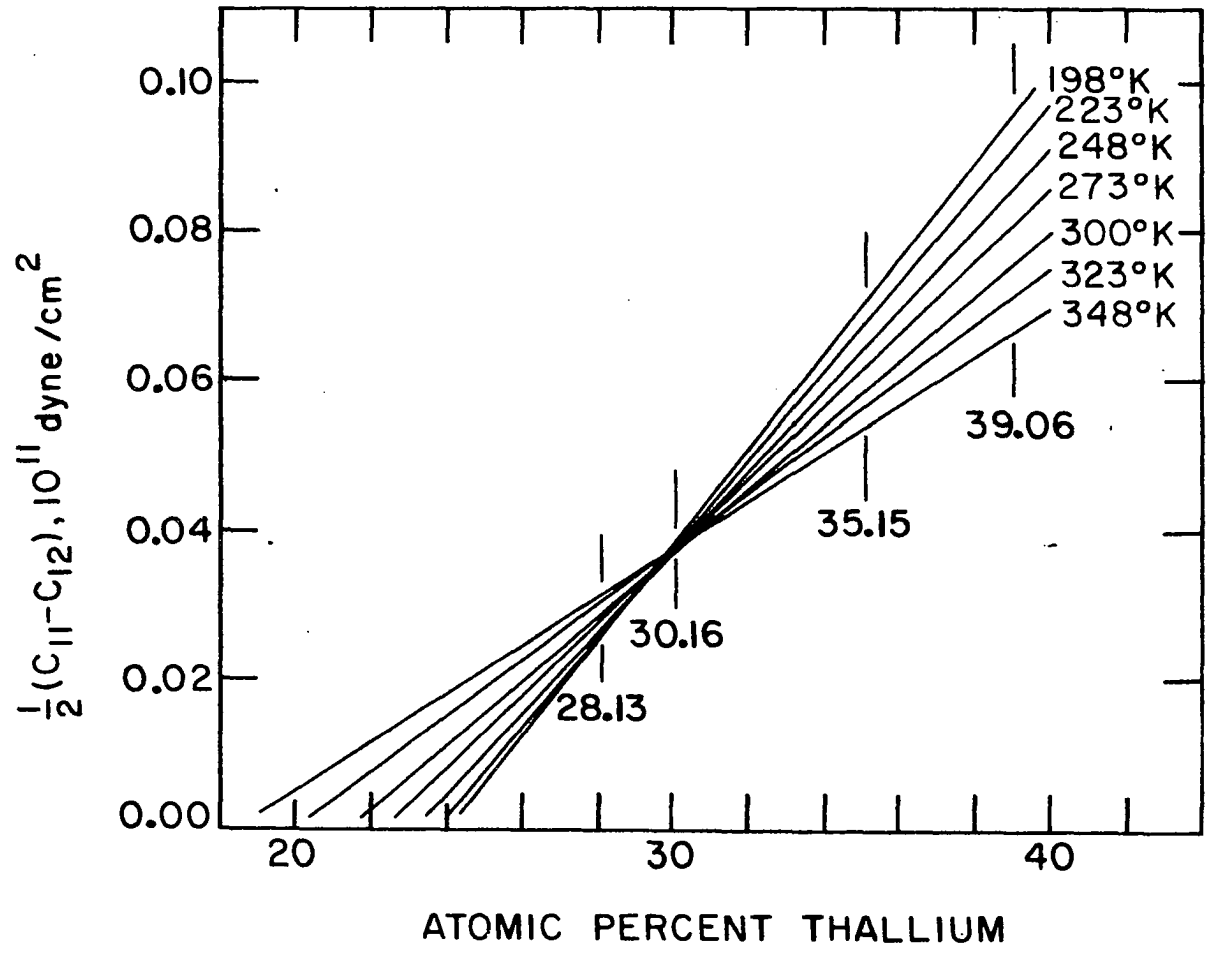

Figure 7. Graphical representation of the equation $C'(T) = A + Bx_{Tl}$

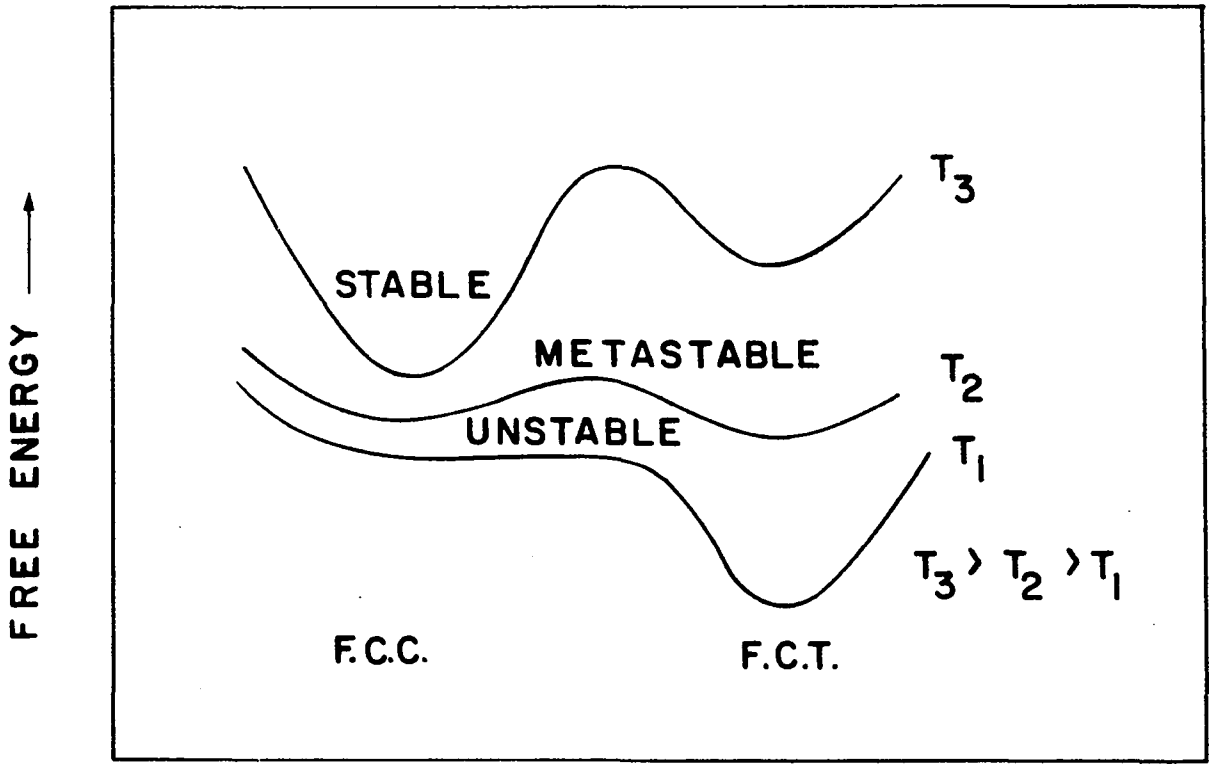

Figure 8. Schematic diagram of the proposed free energy behaviour (after Zener (21))

Interpretation of the Shear Constants

An analysis of the energy terms which account for the values of C' and C_{44} is undertaken in this section. It may be seen from Equations 5 and 6 that the elastic constants can be calculated if the energy of a crystal is known as a function of strain; calculations of the elastic shear constants have been made for the elements of Cu, Al and Mg respectively by Fuchs (22), Leigh (23) and Reitz and Smith (24). In these calculations the energy contributions which account for the values of the shear constants associated with volume conserving shears are a small part of the cohesive energy. At constant volume these terms are the only terms that are functions of shear strain and are represented as the sum

$$W = W(E) + W(I) + W(F) \tag{13}$$

where W(E) is the electrostatic energy of an electrically neutral solid with a lattice of positive point charges embedded in a sea of uniform electron density, W(I) is the repulsive exchange interaction energy between the ion cores and W(F) is the Fermi energy of the valence electrons. The following analysis will show that the terms W(E) and W(I) are inadequate to account for the observed values of the elastic shear constants C_{44} and C'.

Expressions for the contributions to the f.c.c. shear constants C_{44} and C' from the term W(E) were derived by Fuchs (22) who extended Ewald's method (8,25) of calculating the electrostatic energy of a lattice and are

$$C_{44}(E) = 0.9478(2e^2Z^2/a^4) \text{ and } C'(E) = 0.1058(2e^2Z^2/a^4) \quad (14)$$

where a is the lattice parameter in centimeters, e is the charge of an electron in esu, and Z is the number of valence electrons of an atom in the solid. These contributions to the shear constants are the maximum electrostatic contributions and represent the rigidity of a lattice of point charges in a sea of uniform electron density. In a metal the electron distribution is not necessarily uniform and the values of these contributions may be reduced by both a nonuniformity of the actual electron distribution and an additional modulation of the electron distribution caused by the elastic distortion of the lattice (12). The values calculated for the maximum electrostatic contributions with Z = 3 are listed in Table 5.

The contributions to the shear constants from the core-core repulsion term are calculated by representing the repulsive energy per ion pair, u, in the functional form

$$u = Bb \exp((2r_c - r)/\beta) \quad (15)$$

where the distance between nearest neighbor atoms is repre-

Table 5. Calculated and observed values of the cubic elastic constants in units of 10^{11}dyn/cm^2

At. % Tl	Maximum C_{44}(E)	C_{44}(I)	Total C_{44}	Observed C_{44} at 300°K	Maximum C'(E)	C'(I)	Total C'	Observed C' at 300°K
28.13	7.70	0.158	7.86	0.831	0.864	0.034	0.898	0.0291
30.16	7.69	0.160	7.84	0.850	0.855	0.035	0.890	0.0376
35.15	7.64	0.164	7.81	0.867	0.855	0.036	0.891	0.0594
39.06	7.61	0.167	7.77	0.870	0.846	0.037	0.883	0.0758

sented by r and the average radius of the ion cores by r_c. The dependence of the repulsive potential on the charge of the ion is represented by B and is 1.75 for a simple trivalent ion (26). The constants b and β are determined from the lattice constants and compressibilities of ionic solids and are equal to 10^{-12} erg and 0.33×10^{-8} cm respectively (25). The expressions for the contributions of this repulsive energy term to the shear constants of a f.c.c. crystal are calculated by summing the energy per ion pair, u, over all nearest neighbors to find the total repulsive energy per atom W(I). Expressions for the contributions of this repulsive energy to the elastic shear constants are given by Mott and Jones (27) and may be reduced to the following expressions

$$C_{44}(I) = 2y(y - 3)u/a^3 \quad \text{and} \quad C'(I) = y(y - 7)u/a^3 \qquad (16)$$

where $y = r/\beta$. The calculated contributions to the shear constants of the alloys from the core-core interactions are listed in Table 5.

The most striking demonstration that the electrostatic and core-core terms are insufficient to explain the observed values of the elastic constants is seen in the comparison between the experimentally measured and calculated values of the anisotropy ratio illustrated in Figure 6. The value of

this ratio calculated from the maximum electrostatic contributions plus the core-core interactions is 8.8 for all of the alloy compositions. Any effects which reduce the electrostatic contributions to the elastic constants reduce the value of the anisotropy ratio to a minimum of 4.6 for all compositions. This value corresponds to the hypothetical case where no electrostatic contributions are present and is calculated from the core-core repulsion terms alone. Thus, it is seen that the calculated values of the anisotropy ratio do not account for either the observed values of the anisotropy ratio or their rapid change. In conclusion it can be said that the contributions from the Fermi energy to the values of the elastic shear constants are definitely needed to account theoretically for the observed values of these constants.

The Debye Temperature

The Debye theory of lattice vibrations is reviewed in several texts (8,11,27) and relates the Debye temperature, θ, to sonic velocities in an isotropic solid through the relation

$$\theta = \frac{h}{k}\left[\frac{9N\rho}{4\pi M}\right]^{1/3}\left[\frac{2}{v_t^3}+\frac{1}{v_l^3}\right]^{-1/3} \qquad (17)$$

where M is the average atomic weight, v_t and v_l are the

respective velocities of transverse and longitudinal waves, N is Avogadro's number, ρ is the density, h is Planck's constant and k is Boltzmann's constant. Anderson (28) has suggested a simple and approximate method for evaluating the Debye temperature from elastic constant data. In this method the isotropic sonic velocities are calculated from the polycrystalline bulk modulus, K, and shear modulus, G, through the relations

$$v_t = (G/\rho)^{\frac{1}{2}} \quad \text{and} \quad v_l = ((K + 4G/3)/\rho)^{\frac{1}{2}}. \tag{18}$$

The Debye temperature is calculated by substituting the values of these velocities into Equation 17. Table 6 gives the values of G and K at room temperature in units of 10^{11} dyn/cm^2, and θ, in degrees Kelvin, for indium, thallium and the cubic alloys. The values of K and G are the arithmetic mean of the values obtained for each modulus by Voigt and Reuss averaging (12). The uncertainties in the Debye temperatures given in Table 6 were estimated, as suggested by Anderson (28), from the values of G obtained by Voigt and Reuss averaging. The large values of these uncertainties are manifestations of the high degree of elastic anisotropy.

The lower the value of the Debye temperature of a solid the more rapidly the value of its specific heat increases as

its temperature increases from absolute zero. With this in mind it is predicted from the Debye temperatures listed in Table 6 that the specific heats of the alloys will increase more rapidly than the specific heat of indium and should be near the Dulong-Petit value at room temperature. This rapid increase in the specific heat of the alloys is probably due to easily excited transverse vibrational modes in the alloys as indicated by the small values of C'.

Table 6. Values of the shear and bulk moduli at room temperature and the Debye temperatures

At. % Tl	G	K	θ
00.00	0.482[a]	4.18[a]	93 ± 3
28.13	0.290	3.97	66 ± 5
30.16	0.307	4.02	67 ± 5
35.15	0.339	3.99	70 ± 4
39.06	0.359	3.98	71 ± 4
100.00	0.535[b]	3.57[b]	75 ± 2

[a]Values calculated from the data of Winder and Smith (6).

[b]Values calculated from the data of Ferris, Shepard and Smith (7).

The Adiabatic Bulk Modulus

The adiabatic bulk modulus, K, is a thermodynamic property of a solid and for solids with cubic symmetry is related

to the adiabatic elastic constants by the relation

$$K = (C_{11} + 2C_{12})/3 = C_{11} - 4C'/3 \tag{19}$$

The adiabatic bulk modulus of a binary solid solution, K_{sol}, may be related to the adiabatic bulk moduli K_A and K_B of the two respective components A and B of the solid solution. The adiabatic bulk modulus is defined thermodynamically as

$$K = -V(\partial P/\partial V)_S = V(\partial^2 E/\partial V^2)_S \tag{20}$$

where P is pressure, E is internal energy, S is entropy and V is volume. The cohesive energy per gram-atom of a binary solid solution, E_{coh}, can be written, using the law of conservation of energy, as

$$E_{coh} = x_A E_A + x_B E_B - E_f \tag{21}$$

where E_A and E_B are the cohesive energies per gram atom of the pure components, x_A and x_B are the respective mole fractions of the components and E_f is the energy of formation of one gram atom of solid solution. If the assumptions are made that $E_A \gg E_f$, $E_B \gg E_f$ and the gram-atomic volumes of pure A and B are approximately equal to the gram-atomic volume of the solid solution, it follows directly from Equations 20 and 21 that

$$K_{sol} \approx x_A K_A + x_B K_B. \tag{22}$$

In Figure 9 the values, in Table 6, of the polycrystalline bulk moduli of the alloys are plotted as a function of composition along with the polycrystalline bulk moduli of pure indium and thallium. The line in Figure 9 connects the values of the bulk moduli of indium and thallium and is the graphical representation of K_{sol} as expressed in Equation 22. From Figure 9 it may be seen that the experimental points are within 2% of the linear interpolation. An extrapolation of the values of the bulk moduli to pure thallium is justified by the close agreement between this linear interpolation and the values of the bulk moduli. An extrapolated value of $K = 3.57 \times 10^{11}$ dyn/cm^2 was chosen for pure f.c.c. thallium.

Thermodynamically this system is well behaved: the enthalpy change upon mixing liquid indium with liquid thallium may be fit to an analytical expression in which all values are less than 140 cal/g-atom (29), the volume change with alloying at room temperature is essentially ideal (5), and the free energy change at room temperature for the thallium allotropic transformation, f.c.c. → h.c.p., has been estimated (30) to be -18 cal/g-atom which indicated that the free energy change for this transformation in the alloy phases is also very small. In view of the small values of these thermodynamic

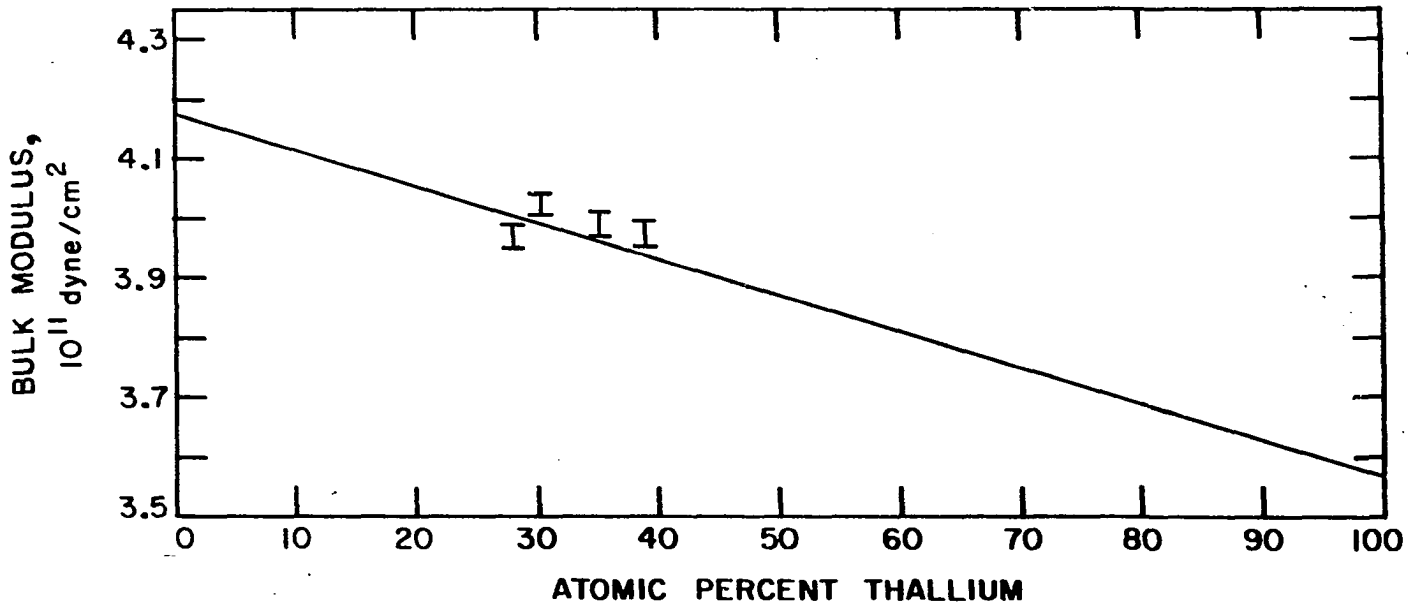

Figure 9. Graphical representation of the bulk moduli of the alloys and pure indium and thallium

quantities it is argued that extrapolations of the shear constants C' and C_{44} to pure thallium will be well behaved. The linear extrapolation of the constant C' by use of Equation 12 for T = 300°K was straightforward and a value of $C' = 0.34 \times 10^{11}$ dyn/cm^2 was obtained for pure thallium. The extrapolation of the values of C_{44} to pure thallium was difficult and could not be done with a high degree of precision because of the fact that no analytical function representing the values of C_{44} outside of the investigated composition range is known. This difficulty was augmented by the small composition range investigated and the long extrapolation required. An extention of the investigated f.c.c. composition range to higher thallium compositions was not possible. This is because the peritectic reaction, shown on the phase diagram in Figure 1, caused the b.c.c. phase to precipitate as the molten alloy was cooled and prevented the growth of a single crystal f.c.c. alloy. An extrapolation of the values of C_{44} at 300°K to pure thallium is shown in Figure 10. Since all the thermodynamic quantities associated with this system are small and well behaved no inflections or peculiarities were expected in this extrapolation. It may further be noted from Figure 10 that the values of C_{44} increase at a

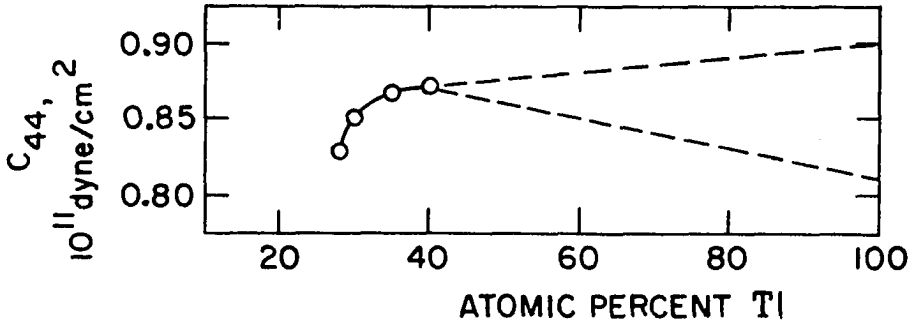

Figure 10. Extrapolation of the values of C_{44} to pure thallium

decreasing rate as the alloys become richer in thallium. In view of these facts the upper limit of the extrapolated value of C_{44} is estimated by a tangential extrapolation and the lower limit is estimated not to be significantly lower than the lowest measured value of C_{44}. The value of $C_{44} = 0.86 \pm 0.05 \times 10^{11}$ dyn/cm^2, which is the mean value of these two limits, was chosen for pure thallium.

Hexagonal and Cubic Thallium

The f.c.c. structure may be thought of as a trigonal structure with the c-axis in one of the <111>-directions. Because of this the cubic elastic constants may be transformed to a trigonal representation and compared directly with the hexagonal elastic constants. The extrapolated values of K and C' at pure thallium can be used to calculate the values of C_{11} and C_{12}. These and the value of C_{44} at pure thallium can be used to calculate the values of the trigonal elastic constants from the relations given in Table 7. The calculated values of the trigonal elastic constants and the values of the hexagonal elastic constants (7) at 300°K are listed in Table 7. The uncertainties given for the values of the trigonal elastic constants were calculated from the uncer-

tainties assigned to the value of C_{44} at pure thallium. It is emphasized that the extrapolations of the cubic moduli to pure thallium are over a long composition range and the uncertainties in the values of the trigonal elastic constants may be much larger than the uncertainties given.

Table 7. Cubic elastic constants in a trigonal representation with the transformed axes: x = $[1\bar{1}0]/\sqrt{2}$, y = $[11\bar{2}]/\sqrt{6}$, and z = $[111]/\sqrt{3}$

Trigonal elastic constants	Trigonal elastic constants in cubic representation	Values at 100 at.% Tl and 300°K[a]	Hexagonal elastic constants at 300°K[b]
C_{11}	$=(C_{11}+C_{12}+2C_{44})/2$	$= 4.54\pm.05$	4.080×10^{11} dyn/cm^2
C_{33}	$=(C_{11}+2C_{12}+4C_{44})/3$	$= 4.71\pm.07$	5.280
C_{44}	$=(C_{11}-C_{12}+C_{44})/3$	$= 0.51\pm.02$	0.726
C_{66}	$=(C_{11}-C_{12}+4C_{44})/6$	$= 0.69\pm.03$	0.270
C_{12}	$=(C_{11}+5C_{12}-2C_{44})/6$	$= 3.17\pm.02$	3.54
C_{13}	$=(C_{11}+2C_{12}-2C_{44})/3$	$= 2.99\pm.03$	2.9
C_{14}	$=(C_{11}-C_{12}-2C_{44})/\sqrt{2}/6$	$= -.24\pm.02$	0.0

[a]Calculated from the values $C_{11} = 4.02$, $C_{12} = 3.34$ and $C_{44} = 0.86 \pm .05 \times 10^{11}$ dyn/cm^2 which were estimated by extrapolation.

[b]Values from the data of Ferris *et al.* (7).

The values of the trigonal elastic constants as compared to the hexagonal elastic constants are consistent with the differences between the crystal dimensions of the two structures. The value of c/a for thallium at 1.598 is less than the ideal value of this ratio. This leads to a larger separation between atoms in the basal planes and a smaller separation between the basal planes of the hexagonal structure than the trigonal structure with the same volume per atom. From this it can be argued that the interatomic forces between the atoms in the basal planes are greater in the trigonal than hexagonal structure. This correlates with the respective values of C_{11} and C_{66} which are greater for the trigonal structure substantiating the prediction that greater interatomic forces exist between atoms in the basal planes of the trigonal structure. Similarily, the spacing between basal planes is less in the hexagonal structure and the respective values of C_{33} and C_{44} are greater for the hexagonal structure.

The values of the trigonal elastic constants of pure thallium are not known with enough precision to make predictions about the relative stabilities of either h.c.p. or f.c.c. thallium. In considering the relative stabilities of different metallic and alloy phases it is found experimentally

that the energy changes associated with structure transformations are generally less than one per cent of the cohesive energies. In conjunction with this, calculations of cohesive energies of these phases are not significantly affected by their structures and cannot be used to predict their most stable structures. In view of the fact that the Fermi energy, which is very sensitive to structure, is a small part of the cohesive energy it may well be that the stabilities of h.c.p. thallium at ambient pressure and of f.c.c. thallium at high pressure are, at least in part, a result of the contribution of the Fermi energies to the cohesive energies of these phases.

The contribution of the Fermi energy to the elastic constants is needed to account for the values of the hexagonal constants C_{44} and C_{66} and is evidenced by the fact that the measured values of these constants for thallium are much smaller than the values calculated for these constants in the hexagonal rare earth metals (31) which are similar to thallium in atomic size and valence. In the calculations of these elastic constants only the electrostatic and core-core interactions were considered. The argument of the Fermi energy being an important factor in accounting for the values of the

elastic constants of hexagonal thallium is strengthened by comparing the measured value of the ratio C_{66}/C_{44} for hexagonal thallium at 0.37 with the theoretically calculated values of this ratio for the hexagonal rare earth metals. These theoretically calculated values range from 2.4 when the maximum electrostatic contributions are considered to a minimum of 0.6 when no electrostatic contributions are considered and at best are twice as large as the measured value for thallium. This substantiates the proposition that the Fermi energy must be an important factor in accounting for the experimental values of the elastic constants of thallium.

SUMMARY

The results of this investigation show that the contribution to the elastic constants from the Fermi energy term is necessary to account theoretically for the observed values of the elastic constants. The values of the Debye temperature calculated from the values of the room-temperature elastic constants indicate a rapid rise in the specific heat of the alloys as their temperature is increased from absolute zero. The room-temperature values of the f.c.c. elastic constants for the alloys are extrapolated to pure thallium. These extrapolated values are used to calculate the values of trigonal elastic constants for pure thallium.

The values of the shear constant, $C' = \frac{1}{2}(C_{11} - C_{12})$, for the alloys could be adequately represented as a function of composition by a linear equation. Extrapolation of these values to zero yielded an absolute stability limit for the indium-rich terminus of the f.c.c. phase field. This stability limit is in excellent agreement with the previously proposed terminus of the indium-rich f.c.c. phase field. The fact that the values of C' vanish as the f.c.c. terminus is approached is consistent with the double shear mechanism proposed for this f.c.c. → f.c.t. transformation.

LITERATURE CITED

1. Hansen, M. Constitution of binary alloys. 2nd ed. New York, N.Y., McGraw-Hill Book Co., Inc. 1958.

2. Burkart, M. W. and Read, T. A. Diffusionless phase change in the indium-thallium system. Trans. Met. Soc. AIME 197, 1516 (1953).

3. Basinski, Z. S. and Christian, J. W. Experiments on the martensitic transformations in single crystals of indium-thallium alloys. Acta Met. 2, 148 (1954).

4. Bridgman, P. W. Polymorphism, principally of the elements, up to 50,000 kg/cm^2. Phys. Rev. 48, 893 (1935).

5. Meyerhoff, R. W. and Smith, J. F. The thallium-indium phase diagram as a function of composition, temperature and pressure. Acta Met. 11, 592 (1963).

6. Winder, D. R. and Smith, Charles S. Single-crystal elastic constants of indium. J. Phys. Chem. Solids 4, 128 (1958).

7. Ferris, R. W., Shepard, M. L. and Smith, J. F. Elastic constants of thallium single crystals in the temperature range 4.2 - 300°K. J. Appl. Phys. 34, 768 (1963).

8. Kittel, Charles. Introduction to solid state physics. 2nd ed. New York, N.Y., John Wiley and Sons, Inc. 1956.

9. Nye, J. F. Physical properties of crystals. London, England, Oxford University Press. 1957.

10. Love, A. E. H. A treatise on the mathematical theory of elasticity. 4th ed. New York, N.Y., Dover Publications, Inc. 1944.

11. de Launay, Jules. The theory of specific heats and lattice vibrations. Solid State Physics 2, 219 (1956).

12. Huntington, H. B. The elastic constants of crystals. Solid State Physics 7, 213 (1958).

13. Lazarus, David. The variation of the adiabatic elastic constants of KCl, NaCl, CuZn, Cu and Al with pressures to 10,000 bars. Phys. Rev. 76, 545 (1949).

14. Eros, S. and Reitz, J. R. Elastic constants by the ultrasonic pulse-echo method. J. Appl. Phys. 29, 683 (1958).

15. Seybolt, A. U. and Burke, J. E. Experimental metallurgy. New York, N.Y., John Wiley and Sons, Inc. 1953.

16. Hildebrand, F. B. Introduction to numerical analysis. New York, N.Y., McGraw-Hill Book Co., Inc. 1956.

17. Smith, J. F. and Schneider, V. L. Anisotropic thermal expansion of indium. J. Less-Common Metals 7, 17 (1964).

18. Meyerhoff, R. W. and Smith, J. F. Anisotropic thermal expansion of single crystals of thallium, yttrium, beryllium, and zinc at low temperatures. J. Appl. Phys. 33, 219 (1962).

19. Guttman, Lester. Crystal-structures and transformations in indium-thallium solid solutions. Trans. Met. Soc. AIME 188, 1472 (1950).

20. Bowles, J. S., Barrett, C. C. and Guttman, L. Crystallography of cubic-tetragonal transformation in the indium-thallium system. Trans. Met. Soc. AIME 188, 1478 (1950).

21. Zener, C. Private communication to C. S. Barrett; cited in Bowles, J. S. and Barrett, C. S. Crystallography of transformations. In Chalmers, Bruce, ed. Progress in metal physics. Vol. 3. pp. 25-26. New York, N.Y., The Macmillan Company. 1961.

22. Fuchs, K. A quantum mechanical calculation of the elastic constants of monovalent metals. Proc. Roy. Soc. (London) A153, 622 (1936).

23. Leigh, R. S. A calculation of the elastic constants of aluminum. Phil. Mag. 42, 139 (1951).

24. Reitz, John and Smith, Charles S. Calculation of the elastic shear constants of magnesium and magnesium alloys. Phys. Rev. 104, 1255 (1956).

25. Born, Max and Huang, Kun. Dynamical theory of crystal lattices. London, England, Oxford University Press. 1954.

26. Seitz, Frederick. Modern theory of solids. New York, N.Y., McGraw-Hill Book Co., Inc. 1940.

27. Mott, N. F. and Jones, H. The theory of the properties of metals and alloys. New York, N.Y., Dover Publications, Inc. 1958.

28. Anderson, Orson L. A simplified method for calculating the Debye temperature from elastic constants. J. Phys. Chem. Solids 24, 909 (1963).

29. Hultgren, R., Orr, R. L., Anderson, P. D. and Kelly, K. K. Selected values of thermodynamic properties of metals and alloys. New York, N.Y., John Wiley and Sons, Inc. 1963.

30. Kaufman, L. Calculation on the effect of pressure on the phase transformations in thallium. Acta Met. 9, 896 (1961).

31. Bernstein, Benjamin T. and Smith, J. F. A calculation of the elastic constants of yttrium and the rare-earth metals. U. S. Atomic Energy Commission Report IS-118 (Iowa State Univ. of Science and Technology, Ames. Inst. for Atomic Research.) 1959.

ACKNOWLEDGEMENTS

The author wishes to express his appreciation to Dr. J. F. Smith for suggesting the problem and for many enlightening discussions throughout the duration of this investigation.